

# Charge redistribution and polarization energy of organic molecular crystals

E.V. Tsiper and Z.G. Soos

*Department of Chemistry, Princeton University, Princeton, NJ 08544*

(June 5, 2001)

We present an approach to electronic polarization in molecular solids treated as a set of quantum systems interacting classically. Individual molecules are dealt with rigorously as quantum-mechanical systems subject to classical external fields created by all other molecules and, possibly, external sources. Self-consistent equations are derived for induced dipoles and for atomic charges whose redistribution in external fields is given explicitly by an atom-atom polarizability tensor. Electronic polarization is studied in two representative organic molecular crystals, anthracene and perylenetetracarboxylic acid dianhydride (PTCDA), and contrasted to previous results for systems of polarizable points. The stabilization energies of the neutral lattice, of isolated anions and cations, and of cation-anion pairs are found. Charge redistribution on ions is included. The dielectric tensors of crystals are successfully related to gas-phase properties and provide consistency checks on polarization energies. The procedure is generally applicable to organic crystals in the limit of no intermolecular overlap.

## I. INTRODUCTION

Recent advances in the preparation of ordered thin films<sup>1</sup> and of organic molecular crystals<sup>2,3</sup> with reduced impurity levels have revived interest in organic electronics and the properties of charge carriers in these materials. Organic molecular crystals are typically insulators with low dielectric constant,  $\kappa \sim 3$ , and charges localized on molecules. Electronic polarization, an effect that is usually not considered in conventional inorganic semiconductors, has a central role in the electronic properties of organic crystals, as discussed by Gutmann and Lyons,<sup>4</sup> Pope and Swenberg,<sup>5</sup> and Silinsh and Capek.<sup>6</sup> When a charge carrier is brought into a molecular solid, its field polarizes the surrounding molecules. Secondary polarization fields created by polarized molecules contribute to the total self-consistent polarization cloud that surrounds each charged quasiparticle. Such a cloud is sometimes referred to as an electronic polaron, to distinguish from lattice relaxation effects.

The overall energy relaxation of a positive and negative charge carrier,  $P_+ + P_-$ , is an important property of an organic material. Typical values<sup>4-6</sup> are in the range of 2–3 eV. The transport gap, i.e. the energy necessary to create a well-separated electron-hole pair is

$$E_t = I - A - P_+ - P_- \quad (1)$$

where  $I$  and  $A$  are the gas-phase ionization potential and electron affinity of the molecule.  $P_+$  and  $P_-$  contain polaronic contributions due to both intramolecular and lattice phonons that are estimated<sup>6</sup> to be  $\sim 10\%$ . We focus on the large *electronic* components of  $P_+$  and  $P_-$  and from now on exclude polaronic effects.

The appearance in Eq. (1) of gas-phase properties is made possible by weak intermolecular forces and Van der Waals separations in organic molecular crystals. The solid-state environment is taken as a perturbation in molecular exciton theory. In contrast to inorganic semiconductors, organic crystals can normally be approxi-

mated as molecules with negligible overlap, and vanishing intermolecular overlap is the crucial approximation to our general development of electronic polarization energies. The energy necessary to create an electron-hole pair at finite separation  $\mathbf{r}$  defines the interaction potential  $V(\mathbf{r}) < 0$ :

$$E_{\text{pair}}(\mathbf{r}) = E_t + V(\mathbf{r}), \quad (2)$$

Nearest-neighbor ion pairs of large molecules obviously deviate from point charges.

Mott and Littleton<sup>7</sup> first estimated the electronic polarization energy in an atomic lattice by considering each atom as a polarizable point. The self-consistent treatment of point charges in lattices of polarizable points was subsequently developed by Munn,<sup>8</sup> Silinsh,<sup>6</sup> and coworkers. While satisfactory for *atomic* lattices, polarizable points for molecules completely neglect their structure. Polarization studies,<sup>6,8</sup> primarily on the acene family, addressed molecular size to some extent by introducing submolecules, whose choice is arbitrary, that carry a fraction of the total molecular polarizability. A recent application<sup>9</sup> to anthracene has several choices, the most elaborate one being submolecules at all carbons, while a study<sup>10</sup> of perylenetetracarboxylic acid dianhydride (PTCDA) has 11 submolecules centered at rings and CO bonds. In effect, the quantum nature of molecules is approximated by the microelectrostatics of submolecules.

In large  $\pi$ -conjugated molecules subject to an external field, charge redistributes over distances comparable to the size of the molecule and generates large nonlinear optical responses. Such a flow of charge in molecules creates secondary polarization fields that do not necessarily reduce to the field of a set of induced dipoles. Thus, rigorous treatment of the polarization field requires analysis of the molecular charge distribution  $\rho(\mathbf{r})$ .

Another issue is electrostatic interactions present already in the ground state of a condensed phase composed of neutral molecules, especially when they contain heteroatoms. These charges induce mutual polarization

in the surrounding molecules and contribute to the overall stabilization energy of the solid. We estimate that the polarization contribution to the ground-state energy can be quite significant, reaching hundreds of meV per molecule. A notable exception is the acene family, whose  $\pi$ -systems have approximate electron-hole symmetry and negligible partial charges, making the polarization energy small.

In this paper we present an approach to electronic polarization in molecular solids that allows for quantitative description of intramolecular charge redistribution. The crucial approximation is the neglect of intermolecular overlap. Zero overlap implies that coordinate space can be subdivided into non-overlapping regions, e.g. Wigner-Seitz cells, associated with individual molecules. Each molecule is then a quantum-mechanical system subject to external fields created by the crystal and, possibly, other external sources. The external fields are rigorously *classical*, so that quantum mechanics is needed at the intramolecular level only.

Section II illustrates the idea and presents self-consistent equations. Section III describes an approximate discrete form of the equations that, we believe, strikes an optimum balance between accuracy and simplicity for practical use. In Sec. IV the equations are applied to the translationally-invariant lattice to find the polarization contribution to the binding energy. In Sec. V equations for the polarization energy of a system of ions embedded in a lattice are derived. The polarization energy of isolated charge carriers in anthracene and PTCDA crystals is calculated, as well as the energy of various ion pairs. The dielectric tensors of anthracene and PTCDA are computed in Sec. VII, and their consistency with polarization energy calculations is established. We compare  $P_+$ ,  $P_-$ , and  $V(\mathbf{r})$  to submolecular results and comment briefly in Sec. VIII on applications to organic solids with mobile charge carriers.

## II. SELF-CONSISTENT CHARGE DISTRIBUTION

In the zero-overlap approximation, the self-consistent solution of the Schrödinger equation for a solid reduces to a product of wave functions of individual molecules. The minimum energy relative to gas-phase (noninteracting) molecules or ions can be done in two steps. First, the change  $E(\phi)$  in the ground state energy of each molecule is found as a functional of the external electrostatic potential  $\phi(\mathbf{r})$ . For simplicity we neglect any magnetic interactions. The ground state charge distribution  $\rho(\mathbf{r}; \phi)$  also depends on  $\phi$  and determines the secondary polarization field created by the molecule.

The total electrostatic potential at a point  $\mathbf{r}$  within a molecule  $a$  is created by all other molecules  $b \neq a$  and, possibly, an applied field:

$$\phi^a(\mathbf{r}) = \phi_{\text{appl}}^a(\mathbf{r}) + \sum_b' \int d^3r' \frac{\rho^b(\mathbf{r}'; \phi^b)}{|\mathbf{r} - \mathbf{r}'|} \quad (3)$$

The prime at the sum excludes the term with  $b = a$ . The total energy of the solid is then

$$E_{\text{tot}} = \sum_a E^a(\phi^a) - \sum_{a < b} \int \int d^3r d^3r' \frac{\rho^a(\mathbf{r}; \phi^a) \rho^b(\mathbf{r}'; \phi^b)}{|\mathbf{r} - \mathbf{r}'|} \quad (4)$$

The second term compensates for double-counting the intermolecular interactions in the first term. Equivalently,

$$E_{\text{tot}} = \sum_a \left[ E^a - \frac{1}{2} \int d^3r (\phi^a - \phi_{\text{appl}}^a) \rho^a \right] \quad (5)$$

Minimization of  $E_{\text{tot}}$  with respect to  $\phi^a(\mathbf{r})$  yields the self-consistent ground state energy of the molecular solid in the approximation of zero overlap.

In principle, variation of Eq. (5) with respect to  $\phi^a$  gives an equation for  $\rho^a(\mathbf{r})$ , which together with Eq. (3) forms a complete self-consistent system. A more efficient way, perhaps, is to use an appropriate quantum chemical procedure to find  $\rho^a(\mathbf{r}; \phi^a)$  for each molecule  $a$  and iterate several times by updating  $\phi^a(\mathbf{r})$  using Eq. (3). The self-consistent problem defined by Eqs. (3) and (5) for charges and potentials is typical of classical electrostatics. The quantum part is limited to the charge distribution  $\rho^a(\mathbf{r}, \phi^a)$ .

The index  $a$  can be dropped or restricted to a single unit cell when the translationally-invariant state of the lattice is of interest. This is the case, for example, in the calculation of the dielectric tensor.<sup>11</sup> Otherwise, a finite number of molecules must be considered. A practical implementation of the procedure requires some form of discretization of the continuous functions  $\phi^a(\mathbf{r})$  and  $\rho^a(\mathbf{r})$  defined within the molecular volume. Certain trade-off between the accuracy and simplicity suitable for repetitive quantum-chemical calculation is unavoidable. In the following section we develop a simple scheme, which captures intramolecular charge redistribution to a quantitative accuracy. The procedure has been successfully implemented by us to calculate indices of refraction of anthracene and PTCDA.<sup>11</sup>

## III. MOLECULE IN NONUNIFORM FIELD

In this section we omit the index  $a$  and consider a single molecule subject to an external potential  $\phi(\mathbf{r})$ . We note that charge redistribution gives a major contribution to the polarizability of large conjugated molecules. This “major part” is not defined quantitatively, as there is no unique definition of atomic charges. The scheme we develop below separates molecular polarizability into two parts, the sum of which matches the actual molecular polarizability  $\alpha$  with the best value known from experiment or theory.

We use a semiempirical Hamiltonian because it provides a natural way to represent an arbitrary external potential acting on a molecule. We define  $\phi_i = \phi(\mathbf{r}_i)$ , the potential at the position of each atom  $\mathbf{r}_i$ . A site energy  $\phi_i$  is added to the diagonal matrix elements for the orthogonalized valence orbitals of atom  $i$ . We employ the INDO/S Hamiltonian,<sup>12</sup> which is known to approximate molecular properties at only a tiny fraction of the cost of *ab-initio* calculations. Throughout the paper we use Löwdin charges  $\rho_i^a$ , where  $i$  labels atoms in molecule  $a$ . The charges are defined as the sums of occupation numbers of orthogonalized orbitals of atom  $i$ .

The corresponding contribution  $\alpha^C$  to the actual polarizability  $\alpha$  is clearly restricted to the molecular plane in conjugated molecules. We associate the difference  $\alpha - \alpha^C$  between the actual and INDO/S polarizabilities with “atomic” contributions caused by the distortion of atomic orbitals in the field. Atomic contributions are small corrections to large in-plane polarizabilities. We note that *any* choice of  $\rho_i(\mathbf{F})$  leads to in-plane  $\alpha^C$  as a consequence of a discrete charge distribution.

Atomic contributions to  $\alpha$  can be described, as in atomic lattices, in terms of induced dipoles situated at the positions of atoms. Based on such an idea we propose the following minimal scheme that is designed to capture both charge-redistribution and “atomic” parts of the molecular response to external fields. We describe the state of an  $N$ -atom molecule by a set of  $2N$  variables,  $\rho_i$  and  $\boldsymbol{\mu}_i$ , which represent the partial charges and induced dipole moments of atoms. The same number of variables,  $\phi_i = \phi(\mathbf{r}_i)$  and  $\mathbf{F}_i = -\nabla\phi(\mathbf{r}_i)$ , describes the external field acting on a molecule.

We denote by  $q_i$  the deviation of partial charges from the ground-state values  $\rho_i^{(0)}$  of an isolated molecule or molecular ion,

$$q_i(\phi) = \rho_i(\phi) - \rho_i^{(0)} \quad (6)$$

At small fields the energy of the molecule is quadratic in the distortion from equilibrium:

$$E(\rho_i, \boldsymbol{\mu}_i; \phi_i, \mathbf{F}_i) = \frac{1}{2} \sum_{ij} q_i \Pi_{ij}^{-1} q_j + \sum_i \rho_i \phi_i + \frac{1}{2} \sum_i \boldsymbol{\mu}_i \tilde{\alpha}_i^{-1} \boldsymbol{\mu}_i - \sum_i \boldsymbol{\mu}_i \mathbf{F}_i \quad (7)$$

Here the positive-definite charge stiffness matrix  $\Pi^{-1}$  describes the increase in the internal energy of the molecule when the charge distribution deviates from its zero-field equilibrium; the tensor  $\tilde{\alpha}_i^{-1}$  plays the same role for atomic dipoles. At given configuration  $\{\phi_i, \mathbf{F}_i\}$  of the external field, the minimum of the energy functional Eq. (7) is achieved at

$$\rho_i = \rho_i^{(0)} - \sum_j \Pi_{ij} \phi_j \quad (8a)$$

$$\boldsymbol{\mu}_i = \tilde{\alpha}_i \mathbf{F}_i, \quad (8b)$$

We see that  $\tilde{\alpha}_i$  is the polarizability for atom  $i$ . It does not necessarily reduce to a scalar, since atoms in a molecule have no rotational symmetry. We could also assume nonzero atomic dipoles  $\boldsymbol{\mu}_i^{(0)}$  in the ground state of nonpolar molecules and so obtain symmetric equations, but we set  $\boldsymbol{\mu}_i^{(0)} = 0$  in this paper.

The energy of the molecule at the minimum is

$$E(\phi, \mathbf{F}) = \sum_i \rho_i^{(0)} \phi_i + \frac{1}{2} \sum_i (q_i \phi_i - \boldsymbol{\mu}_i \mathbf{F}_i). \quad (9)$$

Equivalently,

$$E(\phi, \mathbf{F}) = \sum_i \rho_i^{(0)} \phi_i - \frac{1}{2} \sum_{ij} \phi_i \Pi_{ij} \phi_j - \frac{1}{2} \sum_i \mathbf{F}_i \tilde{\alpha}_i \mathbf{F}_i. \quad (10)$$

The last two terms describe the energy relaxation of the molecule in the external field. The positive-definite symmetric matrix  $\Pi_{ij}$  is the susceptibility with respect to site potentials  $\phi_i$  [cf. Eqs. (8a) and (10)]:

$$\Pi_{ij} = - \left( \frac{\partial \rho_i}{\partial \phi_j} \right)_0 = - \left( \frac{\partial^2 E}{\partial \phi_i \partial \phi_j} \right)_0 \quad (11)$$

Partial derivatives are evaluated at  $\phi_i = 0$ .  $\Pi_{ij}$  determines the charge redistribution among atoms in the external potential. It is a natural extension of the similar quantity  $\pi_{ij}$  used in  $\pi$ -electron theory,<sup>13</sup> and called the atom-atom polarizability. In our case, the total charge of all valence electrons is considered. Note that our definition differs by a factor  $-1/2$ .

Atom-atom polarizabilities  $\Pi_{ij}$  obey the condition

$$\sum_i \Pi_{ij} = \sum_j \Pi_{ij} = 0, \quad (12)$$

since the charge distribution in Eq. (8a) is invariant to an additive constant in all site potentials  $\phi_i$ . The zero-overlap approximation conserves charge at each molecule. Expansion to second order in  $\phi_i$  is sufficient for  $\phi_i < 1$  eV. Eqs. (8) eliminate the need to solve repetitively the quantum problem for the molecule. We calculate  $N(N+1)/2$  atom-atom polarizabilities  $\Pi_{ij}$  only once using Eq. (11) for the neutral molecule and for the cation and anion. Stronger perturbations may require re-evaluation of  $\Pi_{ij}$  at some intermediate  $\phi_i$ .

The total induced moment of a molecule is

$$\boldsymbol{\mu} = \sum_i (\mathbf{r}_i \rho_i + \boldsymbol{\mu}_i). \quad (13)$$

The molecular polarizability consists, therefore, of two terms,  $\alpha = \alpha^C + \tilde{\alpha}$ :

$$\alpha^{\alpha\beta} = \sum_{ij} \Pi_{ij} r_i^\alpha r_j^\beta + \sum_i \tilde{\alpha}_i^{\alpha\beta}. \quad (14)$$

where the Greek indices take the values  $x, y$ , and  $z$ .

Equation (14) illustrates the advantages and limitations of partial atomic charges. With the aid of  $\Pi_{ij}$ , they provide a rigorous description of charge redistribution. The assumption of polarizable points is atomic lattices is kept, however, through  $\tilde{\alpha} = \alpha - \alpha^C$ . We have corrections to INDO/S charges and distribute  $\tilde{\alpha}$  proportionally to the numbers of valence electrons  $n_i$  associated with individual atoms:  $\tilde{\alpha}_i = \tilde{\alpha} n_i / \sum n_i$ . As in previous theory,<sup>6-10</sup>  $\alpha$  is an independent gas-phase input to the calculation.

**Table I** Principal components of the molecular polarizabilities of anthracene and PTCDA; the long (L), medium (M), and normal (N) axes are fixed by  $D_{2h}$  symmetry.

Method	$\alpha_{NN}$ ( $\text{\AA}^3$ )	$\alpha_{MM}$ ( $\text{\AA}^3$ )	$\alpha_{LL}$ ( $\text{\AA}^3$ )
<b>Anthracene</b>			
Experiment <sup>14</sup>	15.2	25.6	35.2
	15.9	24.5	35.9
B3LYP/6-311++G**	12.03	24.27	42.56
INDO/S ( $\alpha^C$ )	0	24.05	41.52
<b>PTCDA</b>			
B3LYP/6-311++G**	18.06	50.27	88.18
INDO/S ( $\alpha^C$ )	0	50.84	84.54

Table I summarizes results for anthracene and PTCDA. Density functional (B3LYP) results have been obtained using the Gaussian 98 program.<sup>15</sup> Theory and experiment are in reasonable agreement for anthracene molecules when large basis sets are used,<sup>11,9</sup> (such as 6-311++G\*\*). Dielectric data<sup>16</sup> for crystalline PTCDA films are also consistent<sup>11</sup> with calculated molecular polarizabilities. The INDO/S results for  $\alpha^C$  from Eq. (14) are confined to in-plane components that represent charge redistribution according to  $\Pi_{ij}$  in Eq. (14). We also need  $\tilde{\alpha} = \alpha - \alpha^C$ . Unless otherwise indicated, we will use the B3LYP polarizabilities in Table I. Since they exceed  $\alpha^C$ , atomic contributions increase the polarization compared to the “charges-only” choice of  $\tilde{\alpha} = 0$ . We note that simple Hückel theory often overestimates responses to applied fields and hence the amount of charge redistribution; in that case  $\tilde{\alpha}$  may be negative and the atomic part reduces the polarization. Equations (8) hold for any  $\tilde{\alpha}$ .

#### IV. SELF-CONSISTENT EQUATIONS

In the condensed phase the potential and field at the position of atom  $i$  of molecule  $a$  created by all other molecules  $b \neq a$  are

$$\phi_i^a = \sum_b \sum_j v(\mathbf{r}_{ij}^{ab}) \rho_j^b + v_\beta(\mathbf{r}_{ij}^{ab}) \mu_j^{b\beta}, \quad (15a)$$

$$F_i^{a\alpha} = \sum_b \sum_j v_\alpha(\mathbf{r}_{ij}^{ab}) \rho_j^b + v_{\alpha\beta}(\mathbf{r}_{ij}^{ab}) \mu_j^{b\beta}, \quad (15b)$$

where  $v(\mathbf{r}) = 1/r$ ,  $v_\alpha(\mathbf{r}) = -\partial v / \partial r^\alpha$ ,  $v_{\alpha\beta}(\mathbf{r}) = \partial^2 v / \partial r^\alpha \partial r^\beta$ . Summation over repeated Greek indices  $\alpha, \beta = x, y, z$  is assumed. The vector  $\mathbf{r}_{ij}^{ab} = \mathbf{r}_i^a - \mathbf{r}_j^b$  points to the atom of interest from atom  $j$  of molecule  $b$ . Here we have assumed no external sources for simplicity. Equations (15) together with Eqs. (8) form a complete self-consistent linear system for  $\rho_i^a$ ,  $\mu_i^a$ ,  $\phi_i^a$ , and  $F_i^a$ .

The total polarization energy of the solid is [compare to Eq. (5)]

$$E_{\text{tot}} = \sum_a \left[ E^a - \frac{1}{2} \sum_i (\rho_i^a \phi_i^a - \mu_i^a F_i^a) \right]. \quad (16)$$

After some algebra and using Eq. (9), this reduces to

$$E_{\text{tot}} = \frac{1}{2} \sum_a \sum_i \rho_i^{a(0)} \phi_i^a. \quad (17)$$

The derivation of this formula is simplified by replacing the dipoles by pairs of charges separated by small distances, and taking the limit in the final expression.

The total energy is a bilinear form of unperturbed charges  $\rho_i^{a(0)}$  and self-consistent potentials  $\phi_i^a$ . We can write it also in terms of self-consistent charges  $\rho_i^a$  and dipoles  $\mu_i^a$ , defining the unperturbed potentials  $\phi_i^{a(0)}$  and fields  $F_i^{a(0)}$  in Eqs. (15) by setting  $\rho_i^a = \rho_i^{a(0)}$  and  $\mu_i^a = 0$ . Using the identity

$$\sum_{ai} \rho_i^{a(0)} \phi_i^a = \sum_{a \neq b} \sum_{ij} v(\mathbf{r}_{ij}^{ab}) \rho_i^{a(0)} \rho_j^b = \sum_{bj} \rho_j^b \phi_j^{b(0)}, \quad (18)$$

the total energy becomes

$$E_{\text{tot}} = \frac{1}{2} \sum_a \sum_i (\rho_i^a \phi_i^{a(0)} - \mu_i^a F_i^{a(0)}). \quad (19)$$

We use this form of  $E_{\text{tot}}$  in Sec. VI to treat ions in infinite lattices.

Equation (19) reduces to the previous result<sup>17,6,8</sup> when all molecules are shrunk to points, with  $\sum_i \rho_i^a = 0$  for molecules and  $\pm 1$  for ions. Since charge redistribution is no longer possible, we may set  $\Pi_{ij} = 0$ ,  $\alpha^C = 0$ , and polarizability  $\tilde{\alpha} = \alpha$  at positions of neutral molecules. The first correction to  $\alpha^C$  for finite molecules is an induced dipole at the center, which gives the same approximation for  $\alpha$  when combined with  $\tilde{\alpha}$ . The potential  $\phi_i^{a(0)}$  in Eq. (19) is due to ions, and the first sum, which is now restricted to charged sites, becomes the source term  $W_0$  of Ref. 17. The second term, over molecules, describes induced dipoles in the field of the ions and is the  $W_1$  term of Ref. 17. The polarizability of ions is generally different from molecules, but is not required for finding  $P_\pm$  in centrosymmetric lattices of point molecules, since the ion is at an inversion center.

The expression (17) or (19) for the lattice polarization energy is not restricted to equivalent molecules. In principle, each molecule  $a$  may have its own  $\rho_i^{a(0)}$ ,  $\Pi_{ij}^a$ , and  $\tilde{\alpha}_i^a$ . In practice, there are several molecules per unit cell in organic molecular crystals. The translationally-invariant lattice of neutral molecules, the neutral lattice of the following section, reduces to atomic charges and potentials within a unit cell. Molecular ions in specified unit cells break translational symmetry and, as discussed in Secs. VI and VII, require different methods for finding  $E_{\text{tot}}$ . In the zero-overlap approximation, charge carriers are molecular ions in place of neutral molecules. The polarization energy  $P_{\pm}$  of a carrier is the energy difference between two extensive quantities, the lattice with the ion and the neutral lattice.

## V. NEUTRAL LATTICE

In this section we evaluate the polarization energy of the neutral lattice. The analogous quantity vanishes identically in the polarizable-point approach, since there are no fields or induced dipoles in the lattice until charges are introduced. The self-consistent Eqs. (8), (15) can be restricted to a single unit cell of volume  $v_c$ . The problem,

$$\mathcal{V}(\mathbf{r}) = -\frac{2\pi r^2}{3v_c} - \frac{\text{erf}(Gr)}{r} + \sum_{\ell}' \frac{1 - \text{erf}(G|\mathbf{r} - \ell|)}{|\mathbf{r} - \ell|} - \frac{\pi}{v_c G^2} + \frac{\pi}{v_c G^2} \sum_{\mathbf{g}}' \frac{\exp(-g^2/4G^2)}{g^2/4G^2} \cos(\mathbf{g}\mathbf{r}), \quad (21)$$

where  $\text{erf}(x) = (2/\sqrt{\pi}) \int_0^x dy \exp(-y^2)$  is the error function. The second sum is over all reciprocal vectors  $\mathbf{g} \neq 0$ ,  $\exp(i\mathbf{g}\ell) = 1$ . Ewald's parameter  $G$  is arbitrary (the result does not depend on its value); a reasonable choice is  $G = (\pi^2/v_c)^{1/3}$ . The function  $\mathcal{V}(\mathbf{r})$  is regular within the central lattice cell  $\ell = 0$ , including the point  $\mathbf{r} = 0$ , and it is not periodic because of the missing term. The function  $\mathcal{V}(\mathbf{r}) + 1/r$  is periodic in  $\mathbf{r}$ .

Equations (15) can be written in terms of  $\mathcal{V}(\mathbf{r})$  and its derivatives  $\mathcal{V}_{\alpha}(\mathbf{r}) = -\partial\mathcal{V}(\mathbf{r})/\partial r^{\alpha}$  and  $\mathcal{V}_{\alpha\beta}(\mathbf{r}) = \partial^2\mathcal{V}(\mathbf{r})/\partial r^{\alpha}\partial r^{\beta}$ :

$$\begin{aligned} \phi_i^a &= \sum_b' \sum_j v(\mathbf{r}_{ij}^{ab}) \rho_j^b + v_{\beta}(\mathbf{r}_{ij}^{ab}) \mu_j^{b\beta} \\ &+ \sum_b' \sum_j \mathcal{V}(\mathbf{r}_{ij}^{ab}) \rho_j^b + \mathcal{V}_{\beta}(\mathbf{r}_{ij}^{ab}) \mu_j^{b\beta}, \end{aligned} \quad (22a)$$

$$\begin{aligned} F_i^{a\alpha} &= \sum_b' \sum_j v_{\alpha}(\mathbf{r}_{ij}^{ab}) \rho_j^b + v_{\alpha\beta}(\mathbf{r}_{ij}^{ab}) \mu_j^{b\beta} \\ &+ \sum_b' \sum_j \mathcal{V}_{\alpha}(\mathbf{r}_{ij}^{ab}) \rho_j^b + \mathcal{V}_{\alpha\beta}(\mathbf{r}_{ij}^{ab}) \mu_j^{b\beta}. \end{aligned} \quad (22b)$$

The sums over  $b$  are restricted to the central unit cell. In the primed sums the term  $b = a$  is excluded. The terms with  $\mathcal{V}$  and its derivatives give contributions by charges and dipoles beyond the central cell.

therefore, reduces to a system of  $4NN_c$  linear equations, where  $N_c$  is the number of molecules in a unit cell, and  $N$  is the number of atoms in a molecule.

Madelung-type infinite sums in Eqs. (15) can be evaluated using Ewald's method.<sup>18</sup> Special care has to be taken to treat complex lattices with many partial charges in a unit cell. For this purpose we introduce a fictitious uniform neutralizing background for each partial charge. Since the unit cell is neutral, these backgrounds cancel exactly. We define an auxiliary potential function  $\mathcal{V}(\mathbf{r})$ ,

$$\mathcal{V}(\mathbf{r}) = \lim_{R \rightarrow \infty} \left[ \sum_{|\ell| < R}' \frac{1}{|\mathbf{r} - \ell|} - \frac{2\pi r^2}{3v_c} - \left( \frac{9\pi M_R^2}{2v_c} \right)^{1/3} \right] \quad (20)$$

where the summation is over  $M_R$  lattice vectors  $\ell$  falling within a sphere of radius  $R$ , with the term  $\ell = 0$  missing. Subtracted is the potential of the uniform neutralizing spherical charge  $-M_R$  centered at the origin of coordinates. Centering of the neutralizing backgrounds at a common point in space is necessary for proper cancellation.

Ewald's method gives

Equations (22) express  $\phi_i^a$  and  $\mathbf{F}_i^a$  in terms of  $\rho_j^b$  and  $\mu_j^b$ . Together with Eqs. (8) they form a complete linear system of  $4NN_c$  equations, half of them vector. For example,  $NN_c = 48$  and  $76$ , respectively, for anthracene and PTCDA lattices, which results in 192 and 304 scalar linear equations for these materials.

The solution for the neutral lattice is further denoted as  $\bar{\rho}_i^a$ ,  $\bar{\mu}_i^a$ ,  $\bar{\phi}_i^a$ , and  $\bar{\mathbf{F}}_i^a$ . These quantities are summed over molecules in Eq. (17) or (19) to yield the (extensive) self-consistent energy of the neutral lattice.

### A. Anthracene and PTCDA

Using the procedure described above we calculated polarization energy of anthracene and PTCDA crystals, which represent two major families of organic semiconductors. Both materials are monoclinic with two molecules per unit cell. Both molecules have centers of inversion and are nearly planar in the crystal. PTCDA molecules are co-planar, up to a small tilt, and form layers and stacks. In anthracene the angle between molecular planes is significant.

We used the X-ray crystal structures for PTCDA<sup>20</sup> and for anthracene<sup>19</sup>. The positions of hydrogens, not given accurately by X-ray, were AM1-optimized using

Gaussian.<sup>15</sup> The gas-phase polarizability, needed to determine the atomic correction  $\tilde{\alpha}$ , is given in Table I.

We obtain polarization energy of 330 meV per PTCDA molecule. This is two orders of magnitude greater than 2.8 meV that we get for anthracene. The large polarization energy of the PTCDA lattice is caused by significant partial atomic charges in neutral PTCDA molecules, which are negligible in anthracene due to the approximate electron-hole symmetry, as mentioned above.

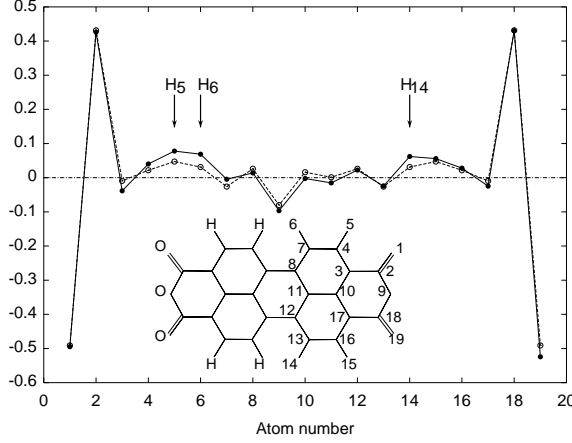


**Fig. 1** Partial charges in PTCDA molecule in crystal lattice ( $\rho_i$ , solid line) and in gas phase ( $\rho_i^{(0)}$ , dashed line)

Figure 1 compares partial atomic charges of a PTCDA molecule in the gas phase and crystal. The inset explains the atom numbering scheme. Only one half of the molecule is shown because of  $C_i$  symmetry. Charge redistribution yields excess positive charge on three hydrogens whose partial charges roughly double. It is worth noticing that these hydrogens reside in positions that suggest the formation of incipient hydrogen bonds; the approximation of zero overlap excludes any covalent contribution. The distances from CH carbons to the nearest oxygen atoms in neighboring molecules are 3.338, 3.269, and 3.768 Å for  $C_5-O_{1'}$ ,  $C_{14}-O_{19'}$ , and  $C_6-O_{19'}$ , respectively, while the corresponding C—H—O angles are 143.8, 149.3, and 158.4° (see Fig. 2).

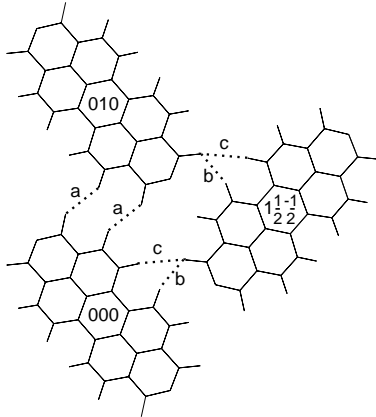


**Fig. 2** Arrangement of PTCDA molecules in a layer [projection onto (102) crystalline plane]. Incipient hydrogen

bonds (dotted lines) involve hydrogen atoms 5(a), 14(b), and 6(c), according to the numbering. Crystalline coordinates here and in Table II conform to the notation of Ref. 20.

## VI. POLARIZATION ENERGY OF CHARGE CARRIERS

We now consider a lattice with one or more neutral molecules replaced with molecular ions. To evaluate the energy, we solve self-consistent equations with the ions and subtract the polarization energy of the neutral lattice. Each ion is described by  $\Pi_{ij}^{ion}$ ,  $\tilde{\alpha}^{ion}$ , and  $\rho_i^{ion(0)}$  ( $\sum \rho_i^{ion(0)} = \pm 1$ ), which may differ from the similar quantities in the neutral molecule. While  $\Pi_{ij}^{ion}$  and  $\rho_i^{ion(0)}$  are determined by semiempirical calculation, the atomic correction  $\tilde{\alpha}^{ion}$  depends on a separate calculation for the ion. In this work, we use the same  $\tilde{\alpha}$  for molecules and ions.

It is useful to rewrite the self-consistent equations (8) and (15) in terms of the deviation from the neutral-lattice solution:

$$\delta\rho_i^a = \rho_i^a - \bar{\rho}_i^a, \quad \delta\phi_i^a = \phi_i^a - \bar{\phi}_i^a, \quad (23a)$$

$$\delta\mu_i^a = \mu_i^a - \bar{\mu}_i^a, \quad \delta F_i^a = F_i^a - \bar{F}_i^a, \quad (23b)$$

The equations for  $\delta\rho_i^a$ ,  $\delta\phi_i^a$ , and each component of  $\delta\mu_i^a$  and  $\delta F_i^a$  then read

$$\delta\rho_i^a = \rho_i^{a*} - \sum_j \Pi_{ij}^a \delta\phi_j^a, \quad (24a)$$

$$\delta\mu_i^{a\alpha} = \tilde{\alpha}_i^{a\alpha} \delta F_i^{a\alpha}, \quad (24b)$$

and

$$\delta\phi_i^a = \sum_b' \sum_j v(\mathbf{r}_{ij}^{ab}) \delta\rho_j^b + v_\beta(\mathbf{r}_{ij}^{ab}) \delta\mu_j^{b\beta}, \quad (25a)$$

$$\delta F_i^{a\alpha} = \sum_b' \sum_j v_\alpha(\mathbf{r}_{ij}^{ab}) \delta\rho_j^b + v_{\alpha\beta}(\mathbf{r}_{ij}^{ab}) \delta\mu_j^{b\beta}. \quad (25b)$$

The source term  $\rho_i^{a*}$  is zero except for ions,

$$\rho_i^{ion*} = \Delta\rho_i^{ion(0)} - \sum_j \Delta\Pi_{ij}^{ion} \bar{\phi}_j^{ion} \equiv \delta\rho_i^{ion}(\bar{\phi}), \quad (26)$$

where  $\Delta\rho_i^{ion(0)} = \rho_i^{ion(0)} - \rho_i^{(0)}$ ,  $\Delta\Pi_{ij}^{ion} = \Pi_{ij}^{ion} - \Pi_{ij}$ , and  $\bar{\phi}_j^{ion}$  is the potential at the ion's position in the lattice. In a hypothetical situation when a neutral molecule is replaced with a foreign molecule which, subject to the potential  $\bar{\phi}_i$ , has charge distribution  $\bar{\rho}_i$ , the source term is zero, and such a molecule will not disturb the translationally-invariant self-consistent solution.

With ions present, the problem has no translational symmetry, and the number of self-consistent equations is infinite. We consider an imaginary cluster within an infinite lattice that includes all the unit cells within a certain

distance  $R$  from the origin. Some dozens of molecules are required for the cluster to resemble a sphere. We set  $\delta\rho_i^a = \delta\mu_i^a = 0$  for the molecules outside the cluster, and solve the self-consistent Eqs. (24) and (25) for  $\delta\rho_i^a$ ,  $\delta\mu_i^a$ ,  $\delta\phi_i^a$ , and  $\delta\mathbf{F}_i^a$  within. This corresponds to an infinite lattice in which only the charges within the cluster are allowed to relax. Molecules outside retain the charge distribution of the neutral lattice.

Setting  $\delta\rho_i^a = \delta\mu_i^a = 0$  does not make  $\delta\phi_i^a$  and  $\delta\mathbf{F}_i^a$  zero outside the cluster. Nevertheless, we can write an expression for the polarization energy of ions that does not contain self-consistent potentials and fields outside the cluster. Subtracting Eq. (19) for the lattice with ions from the similar expression for the translationally-invariant lattice we obtain

$$\begin{aligned} \Delta E_{\text{tot}} = & \frac{1}{2} \sum_a \sum_i (\delta\rho_i^a \phi_i^{a(0)} - \delta\mu_i^a \mathbf{F}_i^{a(0)}) \\ & + \frac{1}{2} \sum_{ion} \sum_i \Delta\rho_i^{ion(0)} \phi_i^{ion}. \end{aligned} \quad (27)$$

The first sum runs over all molecules  $a$  including the ions. The second sum over the ions appears because both  $\rho$ - and  $\phi$ -components of the bilinear expression Eq. (19) are different at  $a = ion$ . The potentials  $\phi_i^{a(0)}$  and fields  $\mathbf{F}_i^{a(0)}$  in the unrelaxed translationally-invariant lattice are evaluated using Eqs. (22) with  $\rho_i^b = \rho_i^{(0)}$  and  $\mu_i^b = 0$ . Thus, Eq. (27) gives the energy of a set of ions in an *infinite* lattice in which molecules beyond the imaginary cluster are not allowed to relax. The polarization energy of the set of ions in an infinite lattice is obtained as  $R \rightarrow \infty$ .

#### A. $P_{\pm}$ in anthracene and PTCDA

We start with a single ion, when Eq. (27) yields either  $P_+$  or  $P_-$  in Eq. (1). The cluster of radius  $R$  is centered on the unit cell that contains the anion or cation. Since clusters are defined in terms of unit cells, we know the number of molecules  $M(R)$  and  $Mv_c/N_c = 4\pi R^3/3$  relates  $R$  to the molecular volume  $v_c/N_c$  in the crystal. The polarization energy  $P_+ + P_-$  for ions at infinite separation is shown in Fig. 3 as a function of  $M^{-1/3}$  for anthracene and PTCDA crystals. The “charges only” points refer to  $\tilde{\alpha} = 0$  and polarization due entirely to charge redistribution; the other points are based on the B3LYP values of  $\alpha$  (Table I). The largest clusters shown in Fig. 3 contain  $M = 2000$  molecules, which corresponds to a cluster diameter of  $2R = 114$  Å for PTCDA and 97 Å for anthracene.

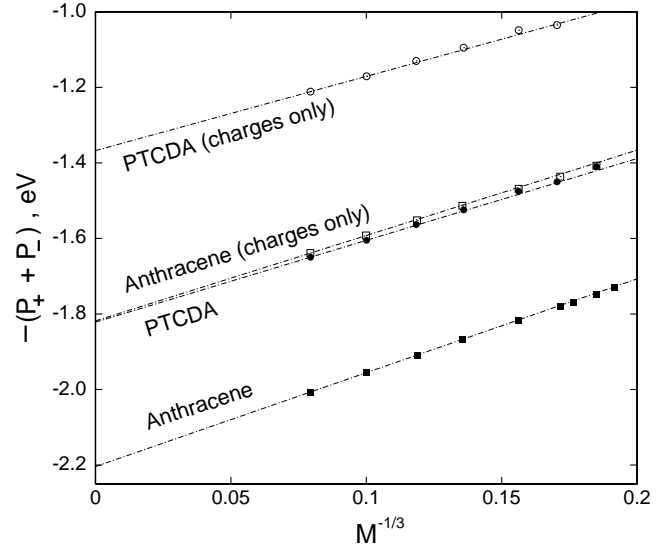


**Fig. 3** Convergence of  $P_+ + P_-$  for anthracene and PTCDA with  $M^{-1/3}$ , which is proportional to the inverse radius  $R^{-1}$  of the cluster. Straight lines are linear fits. Open symbols show the “charges only” results with  $\tilde{\alpha} = 0$ .

The polarization energy decreases with cluster size as more degrees of freedom for charge relaxation are added. At large  $R$  the missing part due to the molecules outside the cluster can be thought of as the polarization energy of a charge in the center of a cavity of radius  $R$  in a continuous dielectric medium. Such energy is linear in  $1/R$ . Linear extrapolation in Fig. 3 gives  $P_+ + P_- = -2.204$  eV for anthracene and  $-1.822$  eV for PTCDA crystals. The smaller ion has the greater stabilization.

The polarization energy of a charge in a spherical cavity in an anisotropic medium has been evaluated by Bounds and Munn<sup>21</sup>

$$P_{\pm}(\infty) - P_{\pm}(R) = -\frac{e^2}{2R} \left( 1 - \frac{1}{\kappa_{\text{eff}}} \right). \quad (28)$$

The effective dielectric constants  $\kappa_{\text{eff}}$  is expressed in terms of the principal values  $\kappa_1 < \kappa_2 < \kappa_3$  of the dielectric tensor

$$\kappa_{\text{eff}} = \frac{\sqrt{\kappa_2(\kappa_3 - \kappa_1)}}{F\left(\arctan \sqrt{\frac{\kappa_3 - \kappa_1}{\kappa_1}}, \sqrt{\frac{\kappa_3(\kappa_2 - \kappa_1)}{\kappa_2(\kappa_3 - \kappa_1)}}\right)} \quad (29)$$

where  $F(\phi, k)$  is the elliptic integral of the first kind. Equations (28) and (29) determine the slope of the asymptotic behavior of  $P_{\pm}$  in Fig. 3. As a consistency check we computed the slope using the dielectric tensor obtained in Sec. VIII. The values 2.482 eVÅ for anthracene and 2.167 eVÅ for PTCDA are within 3% of the slope of the straight line in Fig. 3 drawn through the last two calculated points. The “charges only” slopes are also within 3% of the dielectric constants based on  $\tilde{\alpha} = 0$ .

Submolecules necessarily yield  $P_+ = P_-$ , since ions are assumed to have equal and opposite charges and the

neutral lattice contains neither charges nor dipoles. The anthracene result<sup>21</sup> is  $P_{\pm} = 1.42$  eV for three points at the centers of rings and an effective  $\alpha$  based on the static dielectric tensor of the crystal, while experimental molecular  $\alpha$  yields 1.51 eV for three submolecules. The electronic polarization,  $P_+ + P_- \sim 2.8$  eV, substantially exceeds our 2.20 eV. For PTCDA, 11 submolecules and  $\alpha$  similar to Table I lead to<sup>10</sup>  $P_+ + P_- = 2.14$  eV, which is again greater than our 1.82 eV. While the results clearly depend on the inputted  $\alpha$ , the polarization energy of single ions found via charge redistribution is reduced compared to submolecules, especially when only one or a few are used. The difference is even greater when the ion's charges  $\rho_i^{ion(0)}$  are frozen at the gas-phase values. This decreases  $P_+ + P_-$  by 10–20 % in these systems. Although anthracene and PTCDA ions are at inversion centers, their atoms are not and thus experience local fields that are related by inversion. By contrast, submolecule charges are fixed at the outset and the field vanishes by symmetry at the center of the molecule.

The transport gap, Eq. (1), of molecular crystals is directly related<sup>22</sup> to photoelectron (PES) and inverse photoelectron spectra (IPES) on surfaces, which yield adiabatic  $P_+ + P_-$  that include<sup>6</sup> intramolecular relaxation, but not lattice relaxation. The inferred<sup>22</sup>  $P_+ + P_- \sim 1.7$  eV for PTCDA films is quite consistent with the calculated 1.82 eV in the crystal. The importance of  $E_t$  for electronic organic devices and recent thin film data were the motivation for the accurate calculation of electronic polarization in the well-defined limit of zero overlap. The systems of interest<sup>1–3,22</sup> have mobilities of 0.1–1.0 cm<sup>2</sup>/Vs at room temperature, which is high for organics and indicates that overlap corrections will have to be included.

Partial charges and induced dipoles in the neutral lattice lead to  $P_+ \neq P_-$ . The individual components are shown in Fig. 4 and go as  $M^{-1/3} \propto 1/R$ . The anion and cation slopes are equal at large  $R$ , in accord with Eq. (28).  $P_+$  and  $P_-$  are almost identical for anthracene and strikingly different for PTCDA. In the smallest cluster, which contains only the anion or cation, the ion interacts with the charges  $\bar{\rho}_i$  and dipoles  $\bar{\mu}_i$  of the neutral lattice.

Finite  $P_+(M=1)$  and  $P_-(M=1)$  are the energies of the cation and anion in the unrelaxed neutral lattice. They are nonzero due to fields in the neutral lattice. Without relaxation of the ion itself,  $P_{\pm}(M=1)$  is given by the second term of Eq. (27) with potentials  $\phi_i^{ion} = \bar{\phi}_i + \phi_i^{(0)}$ . The relaxed ion in the field of the neutral lattice has charge distribution  $\rho_i^{ion*}$ , and  $P_{\pm}(M=1)$  is given by Eq. (27) with  $\delta\rho_i^a = \rho_i^{ion*}$  for  $a = ion$  and 0 otherwise. We have assumed  $\tilde{\alpha}^{ion} = \tilde{\alpha}$  for simplicity; more generally, nonzero  $\Delta\tilde{\alpha} = \tilde{\alpha}^{ion} - \tilde{\alpha}$  will introduce a source term  $\mu_i^{ion*} = \Delta\tilde{\alpha}_i \bar{F}_i$  in Eq. (24b).

The large PTCDA contributions at  $M=1$  do not cancel exactly because the anion and cation charges are not precisely equal and opposite. Approximate electron-hole symmetry for the  $\pi$ -system of anthracene ensures almost

equal and opposite charges. Our treatment gives two contributions to  $P_{\pm}$ , an initial interaction at  $M=1$  that does not arise for submolecules and a relaxation or polarization of the lattice that remains almost the same for the anion and cation. Such a distinction may be useful in future work.

The charge distribution in PTCDA is such that positive atomic charges are closer to the molecular centers. The resulting quadrupole moments of molecules create an average positive potential at each molecule in the neutral lattice. The  $\pi$ -electron density above and below the molecular plane also generates a quadrupole as discussed by Silinsh and Capek.<sup>6</sup>

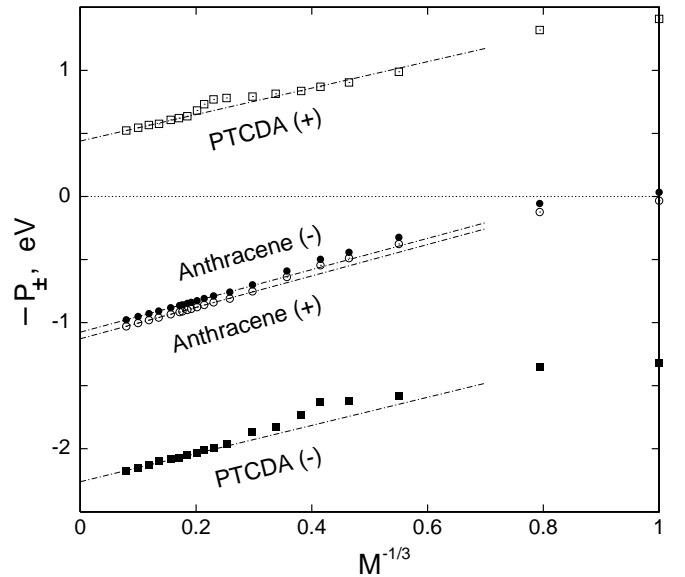


**Fig. 4** Convergence of  $P_+$  and  $P_-$  for anthracene and PTCDA with  $M^{-1/3}$ . Straight lines are linear fits. The values at  $M=1$  are discussed in the text.

In fact, the quadrupole contribution to  $P_+$  and  $P_-$  depends on the macroscopic shape of the sample. It is proportional to  $\int d^3r(1/r^3)$ , which gives finite contribution from the remote parts of the sample. The contribution to the potential is constant on the scale of the unit cell, because the corresponding contribution to the field,  $\propto \int d^3r(1/r^4)$ , vanishes. Thus, the individual quantities  $P_+$  and  $P_-$  are not well defined, but the shape-dependent contribution cancels exactly in the sum,  $P_+ + P_-$ , which enters Eq. (1) for the gap.

The quantities  $I - P_+$  and  $A + P_-$  can be viewed as the ionization potential and the electron affinity of the solid. We see that they depend on the macroscopic shape of the sample due to quadrupolar corrections. In general, the polarization energy of an arbitrary set of charges in a crystal lattice depends on the shape of the macroscopic sample, unless the total charge is zero.

The interpretation of  $P_+$  and  $P_-$  is, however, of considerable interest because PES and IPES spectra are related<sup>22</sup> to  $I - P_+$  and  $A + P_-$ , respectively. Di-



rect comparison, therefore, requires a surface calculation. Compilations<sup>5,6</sup> of  $I - P_+$  for organics, while admittedly approximate, clearly point to  $P_+ > P_-$  and to the physical meaning of individual polarization energies.

### B. Ion pairs in anthracene and PTCDA

Polarization effects modify the interaction between charge carriers. We compute  $V(\mathbf{r})$  in Eq. (2) by replacing two neutral molecules in the lattice with a cation and anion. The cation is at the origin and the anion's center has crystallographic coordinates  $\mathbf{r} = (a,b,c)$  given in Table II. As in the previous section, we consider an imaginary cluster of radius  $R$  that contains both ions, solve the self-consistent Eqs. (24) and (25), and evaluate the energy  $E_{\text{pair}}$  using Eq. (27). We repeat with larger  $R$  until  $V(\mathbf{r})$  converges.

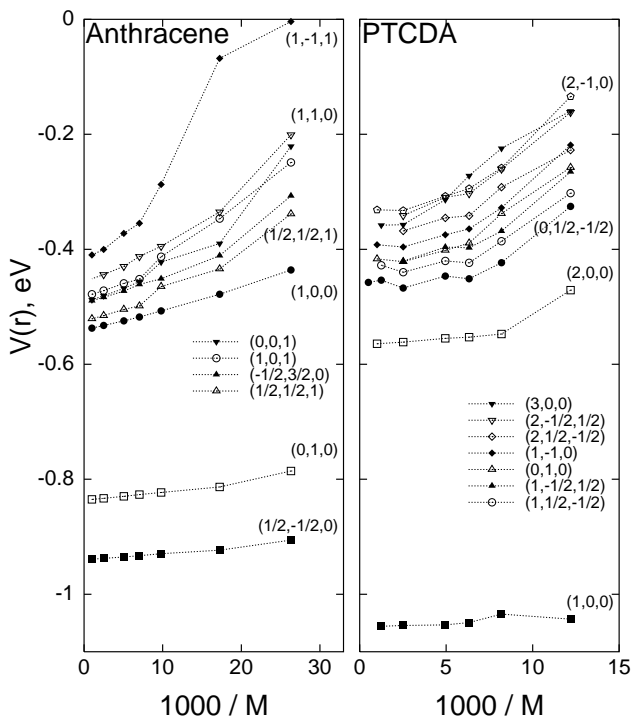


**Fig. 5** Interaction energy  $V(\mathbf{r})$ , Eq. (2), for various ion pairs in clusters of  $M$  molecules.

Figure 5 shows  $V(\mathbf{r})$  as a function of  $1/M$ , which is proportional to the inverse cluster *volume*, for various ion pairs. Since the pair is neutral, the  $1/R$  contribution given by Eq. (28) vanishes, and the asymptotic behavior is linear in  $1/R^3$ . It represents the polarization energy of a dipole in the center of spherical cavity in a dielectric medium.

The extrapolated values of  $V(\mathbf{r})$  for various pairs are presented in Table II, which also lists the distances between centers and identifies pairs using the crystallographic notation of Ref. 20. The lowest charge-transfer

(CT) exciton in PTCDA (Fig. 5) corresponds to neighbors in the stack. The next CT state is the second neighbor along the stack, which is closely followed in energy by other configurations for neighboring molecules in different stacks, as shown in Fig. 2. In anthracene the lowest CT state corresponds to the closest neighbor.

Bounds and Siebrand<sup>23</sup> obtained  $V(\mathbf{r})$  for anthracene using a single point per molecule and experimental polarization data. Their 0.78 and 0.58 eV binding for the lowest CT states are less than our 0.922 and 0.821 eV; the large difference for the second neighbors is due to in-plane polarization and the inadequacy of a single point charge for long molecules that are end-to-end. Anisotropic  $\alpha$  and charge redistribution in anthracene produce several instances (e.g. at 9.894 and 11.172 Å) where  $V(\mathbf{r})$  is not monotonic in  $r$ .

**Table II** Energies  $V(\mathbf{r})$ , in eV, of charge-transfer states within zero-overlap approximation for several separations  $\mathbf{r}$ . The cation and anion are at  $(0,0,0)$  and  $(a,b,c)$  respectively.

Pair $(a,b,c)$	$r$ , Å	$V(\mathbf{r})$	$V_{\text{appr}}(\mathbf{r})^a$
<b>Anthracene</b>			
$(\frac{1}{2}, -\frac{1}{2}, 0)$	5.228	-0.92	-0.79
$(0, 1, 0)$	6.016	-0.82	-0.76
$(1, 0, 0)$	8.553	-0.55	-0.50
$(1, 0, 1)$	9.458	-0.51	-0.50
$(\frac{1}{2}, \frac{1}{2}, 1)$	9.894	-0.54	-0.57
$(-\frac{1}{2}, \frac{3}{2}, 0)$	9.986	-0.51	-0.47
$(1, 1, 0)$	10.456	-0.49	-0.42
$(0, 0, 1)$	11.172	-0.51	-0.56
$(1, -1, 1)$	11.209	-0.50	-0.42
<b>PTCDA</b>			
$(1, 0, 0)$	3.726	-1.06	-0.75
$(2, 0, 0)$	7.453	-0.57	-0.46
$(0, \frac{1}{2}, -\frac{1}{2})$	10.558	-0.46	-0.48
$(1, -\frac{1}{2}, \frac{1}{2})$	10.751	-0.43	-0.40
$(3, 0, 0)$	11.179	-0.38	-0.32
$(1, \frac{1}{2}, -\frac{1}{2})$	11.624	-0.43	-0.46
$(0, 1, 0)$	11.998	-0.42	-0.46
$(2, -\frac{1}{2}, \frac{1}{2})$	12.144	-0.36	-0.32
$(1, -1, 0)$	12.563	-0.39	-0.42
$(2, \frac{1}{2}, -\frac{1}{2})$	13.658	-0.38	-0.37
$(2, -1, 0)$	14.124	-0.33	-0.32

<sup>a</sup> Eq. (30)

The point-charge approximation<sup>24</sup> gives almost 2.0 eV of binding for PTCDA neighbors in a stack, twice the 1.05 eV in Table II, while the binding<sup>10</sup> is 0.99 eV for 11 submolecules. Point charges are poor approximations for large molecules with interplanar separation of 3.4 Å. Charge redistribution and partial charges provide a direct way to compute such electrostatic interactions.

We may consider  $V(\mathbf{r})$  for a cation-anion pair in a continuous anisotropic medium with dielectric tensor  $\kappa$ . We

describe each ion with fixed partial charges  $\rho_i$  and write an electrostatic expression in terms of the double sum over the atoms of the cation and anion. Since  $\Delta E_{\text{tot}}$  is defined relative to the neutral lattice, charge differences  $\Delta\rho_i^{\text{ion}} = \rho_i^{\text{ion}} - \bar{\rho}_i$  appear in  $V(\mathbf{r})$ :

$$V_{\text{appr}}(\mathbf{r}) = \sum_{ij} \frac{\Delta\rho_i^+ \Delta\rho_j^-}{[\det(\kappa) \kappa_{\alpha\beta}^{-1} r_{ij}^\alpha r_{ij}^\beta]^{1/2}}. \quad (30)$$

Here  $r_{ij}^\alpha$  are the components of  $\mathbf{r}_{ij} = \mathbf{r}_i^+ - \mathbf{r}_j^-$ , and  $\det(\kappa) = \kappa_1 \kappa_2 \kappa_3$  is the determinant of the dielectric tensor.<sup>25</sup> At large  $\mathbf{r}$ , Eq. (30) reduces to point charges, since  $\sum_i \bar{\rho}_i = 0$  ensures vanishing interactions in the neutral lattice. The lowest-order corrections to Eq. (30) are induced dipoles due to the other charge.

Table II lists  $V_{\text{appr}}(\mathbf{r})$  values based on Eq. (30) and the dielectric tensors obtained in the next Section. Gas-phase charges and dielectric data are a simple and reasonably accurate approximation to the self-consistent calculation.

We find comparable  $V(\mathbf{r}) \sim -0.5$  eV for second neighbors in PTCDA stacks and first neighbors in different stacks (Fig. 2). Mazur and Petelenz<sup>10</sup> report instead that, by a small margin, an interstack neighbor has binding 1.02 eV that even exceeds the first neighbor. They emphasize the competition between large in-plane polarization for neighbors in adjacent stacks and Coulomb interactions in the same stack. Such trade-offs are seen in Table II for both anthracene and PTCDA, although not as strongly as in Ref. 10. They compute  $E_{\text{pair}}$  for fractional charges at 11 submolecules and then find the Coulomb interaction between the anion and cation using Löwdin charges in a 6-31G basis. While it is inconsistent to use different charges for polarization and direct interactions, it is natural to prefer atomic charges for the anion-cation interaction to arbitrarily placed partial charges.

We also find (1,0,0) to be the lowest CT state by  $\sim 0.3$  eV on using, as in Ref. 10, 11 fractional charges and partial polarizabilities for both the polarization and cation-anion interaction. Hence (1,0,0) is the lowest CT state in PTCDA and, although important, the greater in-plane polarizability does not stabilize neighbors in different chains below (2,0,0).

## VII. DIELECTRIC TENSOR

We now summarize the calculation of the dielectric tensor by considering a sample in a uniform electric field. These results have been reported previously.<sup>11</sup> The procedure is similar to the polarization energy of the neutral lattice in Sec. V.

Formally, an applied field breaks translational invariance, since the electrostatic potential is unbound. Nevertheless, we can add an appropriate constant to the potential in each unit cell and restore translational symmetry, without effect on charge distribution. This follows for

zero overlap because space can be subdivided such that each molecule feels its own potential  $\phi(\mathbf{r})$ . The charge distribution does not change when a constant is added to all  $\phi_i$ , according to Eq. (12).

We add  $E_0^\alpha$  to the right-hand side of Eq. (22b), and the corresponding term  $-r_i^{a\alpha} E_0^\alpha$  to the right-hand side of Eq. (22a). We then solve  $4NN_c$  self-consistent equations (22) and (8), and obtain the total dipole moment  $\boldsymbol{\mu}^a$  of each molecule  $a$  in the unit cell using Eq. (13). The total dipole moment of the unit cell  $\boldsymbol{\mu} = \sum_a \boldsymbol{\mu}^a$  determines the polarization  $\mathbf{P} = \boldsymbol{\mu}/v_c$ , where  $v_c$  is the unit-cell volume. Repeating this procedure with  $\mathbf{E}_0$  directed along each of the coordinate axes we find the tensor  $\zeta$  that relates  $\mathbf{P}$  to  $\mathbf{E}_0$ :

$$\mathbf{P} = \zeta \mathbf{E}_0. \quad (31)$$

Alternatively, one may choose to differentiate the self-consistent equations with respect to  $E_0^\alpha$  to find an explicit expression for  $\zeta$ .

The susceptibility tensor  $\chi$  is defined by the relation  $\mathbf{P} = \chi \mathbf{F}$ , where  $\mathbf{F}$  is the total average macroscopic field that is created by external sources as well as the polarized solid itself.<sup>25</sup> According to the Lorentz relation, a dielectric sphere with uniform polarization  $\mathbf{P}$  creates a field  $-4\pi\mathbf{P}/3$  in its center. The spherical shape is consistent with the definition of  $\mathcal{V}(\mathbf{r})$  in Eq. (21). Thus,

$$\mathbf{F} = \mathbf{E}_0 - \frac{4\pi}{3} \mathbf{P}. \quad (32)$$

Using Eq. (32) we eliminate  $\mathbf{E}_0$  in favor of  $\mathbf{F}$  and using  $\kappa = 1 + 4\pi\chi$  we obtain the dielectric tensor

$$\kappa = \frac{1 + (8\pi/3)\zeta}{1 - (4\pi/3)\zeta} \quad (33)$$

**Table III** Experimental (averaged) and calculated components of dielectric tensor of anthracene and PTCDA

Inputs	$\kappa_1$	$\kappa_b$	$\kappa_3$	$\theta^\circ$
<b>Anthracene</b>				
Experiment <sup>16,26-28</sup>	2.49(10)	3.07(10)	4.04(20)	28(2)
B3LYP/6-311++G**	2.23	2.91	4.03	31.6
Charges only ( $\tilde{\alpha} = 0$ )	1.36	2.39	3.90	34.5
<b>PTCDA</b>				
Experiment <sup>16</sup>	1.9(1)	4.3(2)	4.6(2)	
	1.85	4.07	4.07	
B3LYP/6-311++G**	1.96	3.98	4.02	
Charges only ( $\tilde{\alpha} = 0$ )	1.01	3.74	3.81	

Table III lists the principal components of  $\kappa$  in anthracene crystals and PTCDA films.  $\kappa_2$  is along the  $b$  axis;  $\theta$  is the angle in the  $ac$  plane between  $\kappa_1$  and  $a$ . The anthracene data<sup>16,26-28</sup> are averages over independent measurements of the dielectric tensor and refractive indices. The calculated values are for  $\alpha$  in Table I,

and additional  $\alpha$  inputs for larger bases are reported in Ref. 11. The results agree with the available experimental data, which has an accuracy of a few percent. While  $\tilde{\alpha} = 0$  accounts for  $\kappa_3$ , the largest component, the quantitative importance of accurate  $\alpha$  is clearly seen in Table III.

Equation (33) for  $\kappa$  is strictly based on neutral molecules in a translationally-invariant crystal. The energies of molecular ions were found instead within clusters of radius  $R$ . As noted above, Eq. (28) reproduces the  $M^{-1/3}$  slope in Figs. 3 and 4 within 3%. This demonstrates the internal consistency of the procedure.

### VIII. DISCUSSION

In the limit of zero overlap, molecules in organic crystals are quantum systems with purely classical electrostatic interactions. We have developed a self-consistent approach that treats each molecule quantum-mechanically, subject to the external fields of all other molecules. We have found that such external fields can be treated perturbatively to a good accuracy, expanding the solution of Schrödinger equation for each molecule near the gas-phase solution. Self-consistent analysis of large systems, with over  $10^5$  atoms, is straightforward.

The self-consistent procedure captures an important effect: the redistribution of charge in molecules subject to (nonuniform) external fields. Direct description of charge redistribution avoids the ambiguity that accompanies partitioning the molecular polarizability over a number of polarizable points.

As outlined in Section III, we discretize the molecular charge distribution  $\rho(\mathbf{r})$  by assigning a partial charge  $\rho_i$  and induced dipole  $\boldsymbol{\mu}_i$  to every atom  $i$ . The atom-atom polarizability tensor  $\Pi_{ij}$  then governs charge redistribution in external fields. The tensor  $\Pi_{ij}$  is conveniently found quantum-mechanically at a semiempirical level, such as INDO/S, which is well suited for introducing potentials or site energies. The correction  $\tilde{\alpha} = \alpha - \alpha^C$  is distributed over the atoms, and as in previous theory,<sup>6,8</sup> we still face the familiar problems associated with submolecules. The present approach, however, allows for a certain compensation of error: the partitioning now only involves the small correction  $\tilde{\alpha}$ , which is about 10–20% of the actual molecular polarizability  $\alpha$  in large conjugated molecules.

The electrostatic potential  $\phi(\mathbf{r})$  created by a molecule with charge distribution  $\rho(\mathbf{r})$  is given by Eq. (3). While atomic charges cannot be defined uniquely, charges or dipoles that reproduce  $\phi(\mathbf{r})$  accurately at intermolecular distances in crystals would be completely satisfactory. Thus, *ab-initio*  $\rho(\mathbf{r})$  generate  $\phi(\mathbf{r})$  outside the molecule, which provides a basis<sup>29</sup> for assigning discrete charges. This suggests an interesting possibility of introducing gas-phase atomic dipoles  $\boldsymbol{\mu}_i^{(0)}$  along with the gas-phase atomic charges  $\rho_i^{(0)}$  in Eq. (8b), as long as they improve

the description of fields created by a neutral molecule.

Another possible extension is to introduce atomic quadrupoles to represent  $\pi$ -electron density above and below the plane. This will result in an additional  $10N$  scalar equations per molecule. In practice, only the  $q_{NN}$  component normal to the conjugation plane is needed for  $\pi$ -electrons. Classical multipoles lead to complications even in the limit of no overlap. These are corrections, however, to charges and induced dipoles whose fields  $\mathbf{F}_i$  we have found, and perturbation theory may well be sufficient.

We have already contrasted our method to the existing approach in which a molecule is represented by a number of polarizable points, termed submolecules. The qualitative differences are the electrostatic energy of the neutral lattice and the energy  $P_{\pm}(M=1)$  of an ion in the unrelaxed lattice in Fig. 4. Charge redistribution avoids entirely the number and location of the submolecules. Since the actual  $\alpha$  enters in either case, the numerical results for  $P_+ + P_-$  in Section VI and for  $V(\mathbf{r})$  in Table II do not differ greatly, especially in comparison to calculations with many submolecules.

Crystalline organic films that function as electron or hole conductors are of particular interest for organic electronics.<sup>1–3</sup> Although overlap is then finite, it should be considered as a correction to much greater polarization energies. We have a systematic method for computing the electronic part of  $P_+ + P_-$ , while the total polarization energy in Eq. (1) is about 10% larger due to the lattice contributions, even before overlap or charge transport is introduced. Reliable comparisons of the large electronic part are the first step. We comment on two issues.

First, the greater stabilization of separated ions has major implications on the binding energy  $|V(\mathbf{r})|$  of neighboring ions. Since the energy of the lowest CT in PTCDA<sup>30</sup> is comparable to the lowest Frenkel exciton,  $|V(\mathbf{r})|$  is closely related to discussions and debates about the magnitude of exciton binding energies.<sup>31</sup> Lattice (molecular) relaxation about a separated anion and cation is probably in the range of 200 meV each, while relaxation about an adjacent ion pair is less than 100 meV; the lattice contribution decreases  $|V(\mathbf{r})|$ . Finite overlaps and transfer integrals in the 50–100 meV range are typical for hopping transport and stabilize polarons in Holstein models. CT states, by contrast, have vanishing bandwidth or mobility because two-electron transfers are needed. Overlap also preferentially stabilizes individual ions and hence reduces  $|V(\mathbf{r})|$ . The lowest CT state of PTCDA or anthracene has electronic binding of  $\sim 1$  eV in Table II that could be reduced substantially due to lattice relaxation or by overlap in systems with mobile charges.

The second issue addresses novel features of self-consistent atomic charges. As noted above, charge redistribution of isolated ions increases  $P_+$  or  $P_-$  by about 10% even when ions are at inversion centers. The lower symmetry of ion pairs leads to more extensive charge

redistribution of mutual polarization that is automatically included in our treatment through  $\Pi_{ij}$  for ions. Charge redistribution on ions is important. Its contribution can be estimated by self-consistent calculation with ionic charges and dipoles set to gas-phase values. Specific contributions are found by comparing two self-consistent solutions.

In summary, we have implemented a general approach to electronic polarization of organic molecular crystals in the limit of zero intermolecular overlap. Redistribution of partial atomic charges is governed by the atom-atom polarizability tensor  $\Pi_{ij}$ , which provides a quantum mechanical basis for the description of electronic polarization. Partial charges replace the microelectronics of postulated submolecules in previous treatments and introduce such new features as electronic stabilization of the neutral lattice and charge relaxation on ions. Self-consistent atomic charges and induced dipoles relate the molecular polarizability of anthracene or PTCDA to the dielectric tensor and the energies of fixed ions and ion pairs in the crystal. The cluster approach used for ions is suitable for surfaces and other systems with reduced symmetry, provided that all molecular positions are specified. Zero overlap provides a starting point for the treatment of electronic polarization in organic systems with mobile localized charge carriers.

## ACKNOWLEDGMENTS

It is a pleasure to thank R.A. Pascal, Jr., for discussions and assistance with structural data and molecular polarizabilities; A. Kahn, S.F. Forrest, M. Hoffmann, and J.M. Sin for discussions of transport gaps, PES spectra, CT excitons and atomic charges; and P. Petelenz and R.W. Munn for correspondence about induced dipoles. This work was partly supported by the National Science Foundation through the MRSEC program under DMR-9400362.

<sup>1</sup> S.R. Forrest, Chem. Rev. **97**, 1793 (1997) and references therein.

<sup>2</sup> J.H. Schön, C. Kloc, and A. Dodabalapur, Science **289**, 599 (2000).

<sup>3</sup> J.H. Schön, C. Kloc, and B. Batlogg, Science **288**, 2338 (2000).

<sup>4</sup> F. Gutmann and L.E. Lyons, Organic Semiconductors, (Wiley, New York, 1967) Ch. 6

<sup>5</sup> M. Pope and C.E. Swenberg, *Electronic Processes in Organic Crystals* (Clarendon, Oxford, 1982).

<sup>6</sup> E.A. Silinsh and V. Capek, *Organic Molecular Crystals:*

*Interaction, Localization and Transport Phenomena* (Am. Inst. Phys., New York, 1994).

- <sup>7</sup> N.F. Mott and M.J. Littleton, Trans. Faraday Soc. **34**, 485 (1938).
- <sup>8</sup> J.W. Rohleder and R.W. Munn, Magnetism and Optics of Molecular Crystals (Wiley, New York, 1992) and references therein.
- <sup>9</sup> H. Reis, M.G. Papadopoulos, P. Calaminici, K. Jug and A.M. Köster, Chem. Phys. **261**, 359 (2000); H. Reis, M.G. Papadopoulos, and D.N. Theodorou, J. Chem. Phys. **114**, 876 (2001).
- <sup>10</sup> G. Mazur and P. Petelenz, Chem. Phys. Lett. **324**, 161 (2000).
- <sup>11</sup> Z.G. Soos, E.V. Tsiper, and R.A. Pascal, Jr., in press.
- <sup>12</sup> M.C. Zerner, G.H. Loew, R.F. Kirchner, and U.T. Mueller-Westerhoff, J. Am. Chem. Soc., **102**, 589 (1980).
- <sup>13</sup> C.A. Coulson and H.C. Lonquet-Higgins, Proc. Roy. Soc. (London) **A191**, 39 (1947); L. Salem, *The Molecular Orbital Theory of Conjugated Systems* (Benjamin, New York, 1966), Ch. 1.
- <sup>14</sup> C.L. Cheng, D.S.N. Murthy, and G.L.D. Ritchie, Austr. J. Chem. **25**, 1301 (1972); R.J.W. LeFevre, L. Radom, and G.L.D. Ritchie, J. Chem. Soc. B., 775 (1968).
- <sup>15</sup> M.J. Frisch et al., GAUSSIAN 94 (Gaussian Inc, Pittsburgh, 1995).
- <sup>16</sup> D.Y. Zang, F.F. So, and S.R. Forrest, Appl. Phys. Lett. **59**, 823 (1991).
- <sup>17</sup> D. Fox, Chem. Phys. **17**, 273 (1979).
- <sup>18</sup> E. Madelung, *Die Mathematischen Hilfsmittel Des Physikers*, Berlin, Springer-Verlag (1957); M. Born and M. Bradburn, Proc. Cambridge Phil. Soc. **39**, 104 (1943).
- <sup>19</sup> C.P. Brock and J.D. Dunitz, Acta Crystallogr **B46**, 795 (1990).
- <sup>20</sup> T. Ogawa, K. Kuwamoto, S. Isoda, T. Kobayashi, and N. Karl, Acta Crystallogr. **B55**, 123 (1999).
- <sup>21</sup> P.J. Bounds and R.W. Munn, Chem. Phys. **44**, 103 (1979).
- <sup>22</sup> I.G. Hill, A. Kahn, Z.G. Soos, and R.A. Pascal, Jr., Chem. Phys. Lett. **327**, 181 (2000).
- <sup>23</sup> P.J. Bounds and Siebrand, Chem. Phys. Lett. **75**, 414 (1980).
- <sup>24</sup> Z. Shen and S.R. Forrest, Phys. Rev. **B55**, 10578 (1997).
- <sup>25</sup> L.D. Landau and I.M. Lifshitz, *Electrodynamics of continuous media* (Oxford; New York: Pergamon, 1993).
- <sup>26</sup> N. Karl, H. Rohrbacher, and D. Siebert, Phys. Status Solidi **A4**, 105 (1971).
- <sup>27</sup> R.W. Munn, J.R. Nicholson, H.P. Schwob, and D.F. Williams, J. Chem. Phys. **58**, 3828 (1973).
- <sup>28</sup> A.N. Winchell, *The Optical Properties of Organic Compounds*, 2nd ed., (Acad. Press, New York, 1954).
- <sup>29</sup> M.M. Francl and L.E. Chirlian, Rev. Comp. Chem. **14**, 1 (2000).
- <sup>30</sup> M.H. Hennessy, R.A. Pascal, Jr., and Z.G. Soos, Mol. Cryst. Liquid. Cryst. **335**, 41 (2001); M.H. Hennessy, Z.G. Soos, R.A. Pascal, Jr., and A. Girlando, Chem. Phys. **245**, 199 (1999).
- <sup>31</sup> *Primary photoexcitations in conjugated polymers: Molecular exciton versus semiconductor band model*, Ed. by N.S. Sariciftci, (World Scientific, Singapore, 1997)